

A fast and oblivious matrix compression algorithm for Volterra integral operators

J. Dölz · H. Egger · V. Shashkov

the date of receipt and acceptance should be inserted later

Abstract The numerical solution of dynamical systems with memory requires the efficient evaluation of Volterra integral operators in an evolutionary manner. After appropriate discretisation, the basic problem can be represented as a matrix-vector product with a lower diagonal but densely populated matrix. For typical applications, like fractional diffusion or large scale dynamical systems with delay, the memory cost for storing the matrix approximations and complete history of the data then would become prohibitive for an accurate numerical approximation. For Volterra-integral operators of convolution type, the *fast and oblivious convolution quadrature* method of Schädle, Lopez-Fernandez, and Lubich allows compute the discretized evaluation with N time steps in $O(N \log N)$ complexity and only requiring $O(\log N)$ active memory to store a compressed version of the complete history of the data. We will show that this algorithm can be interpreted as an \mathcal{H} -matrix approximation of the underlying integral operator and, consequently, a further improvement can be achieved, in principle, by resorting to \mathcal{H}^2 -matrix compression techniques. We formulate a variant of the \mathcal{H}^2 -matrix vector product for discretized Volterra integral operators that can be performed in an evolutionary and oblivious manner and requires only $O(N)$ operations and $O(\log N)$ active memory. In addition to the acceleration, more general asymptotically smooth kernels can be treated and the algorithm does not require a-priori knowledge of the number of time steps. The efficiency of the proposed method is demonstrated by application to some typical test problems.

J. Dölz
Institute for Numerical Simulation, University of Bonn, Friedrich-Hirzebruch-Allee 7, 53115 Bonn, Germany. E-mail: doelz@ins.uni-bonn.de

H. Egger
Numerical Analysis and Scientific Computing, Department of Mathematics, TU Darmstadt, Dolivostr. 15, 64293 Darmstadt, Germany. E-mail: egger@mathematik.tu-darmstadt.de

V. Shashkov
Numerical Analysis and Scientific Computing, Department of Mathematics, TU Darmstadt, Dolivostr. 15, 64293 Darmstadt, Germany. E-mail: shashkov@mathematik.tu-darmstadt.de

1 Introduction

We study the numerical solution of dynamical systems with memory which can be modelled by abstract Volterra integro-differential equations of the form

$$\alpha(t)y'(t) + A(t)y(t) = \int_0^t k(t,s)f(s,y(s)) ds, \quad 0 \leq t \leq T. \quad (1)$$

Such problems arise in a variety of applications, e.g., in population growth models, anomalous diffusion, option pricing, neural sciences, transparent boundary conditions, wave propagation, field circuit coupling, or the coarse-graining of soft-matter systems; see e.g. [1, 6, 7, 11, 12, 19, 25, 28, 30] and the references therein. The simplest model problem already sharing the essential difficulties stemming from non-locality of the right hand side in (1) is the evaluation of the integral operator

$$y(t) = \int_0^t k(t,s)f(s) ds, \quad 0 \leq t \leq T, \quad (2)$$

with kernel function k , data f , and result function y . Let us emphasize that, in order to allow the application in the context of integro-differential problems (1), the parameter-dependent integrals (2) have to be evaluated in an *evolutionary* manner, i.e., for successively increasing time.

1.1 Discretisation and related work

After applying some appropriate discretisation procedure, problem (2) can be phrased as a simple matrix-vector multiplication

$$\mathbf{y}_n = (\mathbf{K}\mathbf{f})_n, \quad 1 \leq n \leq N. \quad (3)$$

The evolutionary character and the nonlocal interactions are then reflected by the fact that the matrix $\mathbf{K} \in \mathbb{R}^{N \times N}$ is lower block triangular but densely populated. The straight-forward computation of the result vector \mathbf{y} then requires $O(N^2)$ algebraic operations. The evolutionary character of problem (2) can be preserved by computing the entries \mathbf{y}_n for $n = 1, \dots, N$ recursively, i.e., by traversing the matrix \mathbf{K} from top to bottom. On the other hand, if the matrix \mathbf{K} is traversed from left to right, then the algorithm becomes *oblivious*, i.e., the data \mathbf{f}_n is only required in the n th step of the algorithm, but the execution of (3) then requires $O(N)$ active memory to store the partial sums for every row. Although the evaluation can then still be organized in an evolutionary manner, see section 2.2, the number of time steps N needs to be fixed *a-priori* in order to store the intermediate results.

For the particular case that integral kernel in (2) is of convolution type, i.e.

$$k(t,s) = k(t-s), \quad (4)$$

a careful discretisation of (5) gives rise to an algebraic system (3) with block Toeplitz matrix \mathbf{K} , and the discrete solution \mathbf{y} can be computed in $O(N \log N)$ operations using fast Fourier transforms. As shown in [20], an evolutionary computation can be realized in $O(N \log^2 N)$ complexity and requiring $O(N)$ active memory. The convolution quadrature methods introduced of [23, 24, 26] treat the

case that only the Laplace transform $\hat{k}(s)$ of the convolution kernel (4) is available. The *fast and oblivious convolution quadrature* method introduced in [22, 27] allows the efficient evaluation of Volterra integrals with convolution kernel in an *evolutionary* and *oblivious* manner with $O(N \log N)$ operations and only $O(\log N)$ active memory and $O(\log N)$ evaluations of the Laplace transform $\hat{k}(s)$. This method has been applied successfully for the numerical solution of partial differential equations with transparent boundary conditions [19], boundary element methods for the wave equation [30] or fractional diffusion [8].

For integral operators (2) with general kernels $k(t, s)$, the above mentioned methods cannot be applied directly, but alternative approaches, like the fast multipole method [13, 15, 29], the panel clustering technique [18], \mathcal{H} - and \mathcal{H}^2 -matrices [4, 16], multilevel techniques [5, 14] or wavelet algorithms [9], which were developed and applied successfully in the context of molecular dynamics and boundary integral equations, are still applicable. These methods are based on certain hierarchical approximations for the kernel function $k(t, s)$, whose error can be controlled under appropriate smoothness assumptions. If the data f is independent of the solution y , the numerical evaluation of the Volterra-integral operator (2) can then be realized with $O(N \log^\alpha N)$ computational cost with some $\alpha \geq 0$ and N denoting the dimension of the underlying discretisation. Moreover, data-sparse approximations of the matrix \mathbf{K} for general kernels $k(t, s)$ can be stored efficiently with only $O(N \log^\alpha N)$ memory and for convolution kernels $k(t - s)$ even with $O(\log N)$ memory; we refer to [4, 17] for details and an extensive list of references. Unfortunately, the algorithms mentioned in literature are not evolutionary and, therefore, cannot be applied to more complex problems like (1) directly.

1.2 A fast and oblivious evolutionary algorithm

In this paper, we propose an algorithm for the evaluation of Volterra integrals (2) or the corresponding matrix-vector products (3) which shares the benefits and overcomes the drawbacks of the approaches mentioned above, i.e., it is

- *evolutionary*: the approximations y_n can be computed one after another and the number of time steps N does not need to be known in advance,
- *oblivious*: the entry f_n of the right hand side is only required in the n th step,
- *fast*: the evaluation of all y_n , $1 \leq n \leq N$ requires $\mathcal{O}(N)$ operations, and
- *memory efficient*: the storage of the convolution matrix only requires $\mathcal{O}(N)$ storage for instationary and $\mathcal{O}(\log(N))$ storage for stationary convolution kernels. The matrix entities can also be computed on the fly, such that only $\mathcal{O}(\log(N))$ storage is required to store a compressed history of the data f .

Our strategy is based on the ideas of polynomial-based \mathcal{H}^2 -compression algorithms to find a hierarchical low-rank approximation of the kernel function $k(t, s)$ leading to a block-structured hierarchical approximation of the matrix \mathbf{K} . The accuracy of the underlying approximation can thus be guaranteed by well-known approximation results; see [4, 17] for instance. A key ingredient for our results is the one-dimensional nature of the integration domain which allows to characterize the block structure of the approximating hierarchical matrix very explicitly. This allows us to formulate an algorithm which traverses the compressed matrix in (3)

from top-to-bottom in accordance with the evolutionary structure of the underlying problem. The hierarchical approximation of the convolution kernel also yields a compression strategy for the history of the data f . In this sense, our algorithm can be considered a generalisation to [3], where a multipole expansion was employed in the special context of fractional time derivatives, and to [21], where a polynomial on growing time steps was employed for the compression of the data.

As a further result, we show that our algorithm seamlessly integrates into the convolution quadrature framework of [23,24], when the kernel $k(t-s)$ is of convolution type (4) and only accessible via its Laplace transform. In analogy to the treatment of nearfield contributions in the fast boundary element method, we utilize standard convolution quadrature to compute the entries of the convolution matrix (3) close to the diagonal, while advanced numerical methods for the Laplace inversion [10] are used to setup an \mathcal{H}^2 -approximation of the remaining off-diagonal parts of the convolution matrix. Although this approach has some strong similarities to the fast and oblivious convolution quadrature method [27,31], we will reveal some subtle but important differences. In particular, we illustrate that the methods of [27,31] can actually be interpreted as \mathcal{H} -matrix approximations with a particular organisation of the matrix-vector product (3). This shows that the $\mathcal{O}(N \log N)$ complexity cannot be further improved. Moreover, the convolution matrix must be applied from left to right to allow for an oblivious evaluation and the number of time steps N must be known in advance. In contrast to that, our new algorithm is based on an \mathcal{H}^2 -approximation of the convolution matrix. The evolutionary, fast and oblivious evaluation of the matrix-vector product can be realized by traversing through the matrix from top to bottom in $\mathcal{O}(N)$ complexity and without needing to know the number of time steps N in advance. Finally, our algorithm naturally extends to general integral kernels $k(t, s)$.

1.3 Outline

The rest of the manuscript is organized as follows: In Section 2 we recall some general approximation results, introduce our basic notation, and state a slightly modified algorithm for the dense evaluation of the Volterra integral operators to illustrate some basic principles that we exploit later on. Section 3 is concerned with a geometric partitioning on the domain of integration, the multilevel hierarchy used for the \mathcal{H}^2 -compression, and the description and analysis of our new algorithm. In Section 4 we consider convolution kernels $\hat{k}(s)$ and discuss the relation of our algorithm to Lubich's convolution quadrature and the connections to the fast and oblivious algorithm of [27,31]. To support our theoretical considerations, some numerical results are provided in Section 5.

2 Preliminary results

Let us start with summarizing some basic results about typical discretisation strategies for Volterra integral operators

$$y(t) = \int_0^t k(t, s) f(s) ds \quad (5)$$

which are the basis for the efficient and reliable numerical evaluation later on. For simplicity, all functions y , f , and k are assumed to be scalar valued. We will demonstrate the application to more general problems of the form (1) in Section 5.

2.1 A general approximation result

For the discretisation of the integral operator (5), we consider methods of the form

$$\tilde{y}_h(t) = \int_0^t k_h(t, s) f_h(s) ds, \quad (6)$$

where k_h and f_h are suitable approximations for k and f . The subscript h will be used to designate approximations throughout. The following result may serve as a theoretical justification for a wide variety of particular discretisation schemes.

Lemma 1 *Let $T > 0$, kernels $k, k_h \in L^\infty(0, T; L^r(0, T))$, and $f, f_h \in L^{r'}(0, T)$ be given with $1 \leq r, r' \leq \infty$ with $1/r + 1/r' = 1$. Further assume that*

$$\|k - k_h\|_{L^\infty(0, T; L^r(0, T))} \leq \varepsilon \quad \text{and} \quad \|f - f_h\|_{L^{r'}(0, T)} \leq \varepsilon. \quad (7)$$

Then the functions y, \tilde{y}_h defined by (5) and (6) satisfy

$$\|y - \tilde{y}_h\|_{L^\infty(0, T)} \leq C(\|k\|_{L^1(0, T; L^r(0, T))} + \|f\|_{L^{r'}(0, T)} + \varepsilon)\varepsilon, \quad (8)$$

i.e., the error in the results can be bounded uniformly by the perturbation in the data.

Proof From Hölder's inequality, we can deduce that

$$\begin{aligned} |y(t) - \tilde{y}_h(t)| &\leq \int_0^t |k(t, s)| |f(s) - f_h(s)| + |k(t, s) - k_h(t, s)| |f_h(s)| ds \\ &\leq \|k(t, \cdot)\|_{L^r(0, T)} \|f - f_h\|_{L^{r'}(0, T)} + \|k(t, \cdot) - k_h(t, \cdot)\|_{L^r(0, T)} \|f_h\|_{L^{r'}(0, T)}. \end{aligned}$$

The result then follows by estimating $\|f_h\| \leq \|f\| + \|f - f_h\|$, using the estimates for the differences in the data, and taking the supremum over all $0 < t < T$.

Remark 1 The constant C in the estimate (8) depends on the kernel k , but is independent of T . The result can therefore be applied to time intervals of arbitrary size. Without substantially changing the argument, it is possible to obtain similar estimates also in other norms. In many cases, \tilde{y}_h only serves as an intermediate result and the final approximation is given by $y_h(t) = (P_h \tilde{y}_h)(t)$, where P_h is some projection or interpolation operator; a particular case will be discussed in more detail below. Estimates for the error $\|y - y_h\|$ can then be obtained by additionally taking into account the projection errors.

2.2 Piecewise polynomial approximations

Many discretisation methods for integral or integro-differential equations, e.g., collocation or Galerkin methods, are based on piecewise polynomial approximations and fit into the abstract form mentioned above. As a particular example and for later references, we consider such approximations in a bit more detail now.

Let $h > 0$ be given, define $t^n = nh$, $n \geq 0$, and set $T = t^N = Nh$. We set $I^n = [t^{n-1}, t^n]$ for $1 \leq n \leq N$, and denote by $\mathcal{T}_h = \{I^n : 1 \leq n \leq N\}$ the resulting uniform mesh of the interval $[0, T]$. We further define piecewise polynomial spaces

$$\mathcal{P}_p(\mathcal{T}_h) = \{f \in L^1(0, T) : f|_{I^n} \in \mathcal{P}_p(I^n)\}, \quad (9)$$

$$\mathcal{P}_{q,q}(\mathcal{T}_h \times \mathcal{T}_h) = \{k \in L^1((0, T) \times (0, T)) : k|_{I^m \times I^n} \in \mathcal{P}_{q,q}(I^m \times I^n)\}, \quad (10)$$

over the grid \mathcal{T}_h and the tensor-product grid $\mathcal{T}_h \times \mathcal{T}_h$. We write $\mathcal{P}_p(a, b)$ for the space of polynomials of degree at most p , and $\mathcal{P}_{q,q}((a, b) \times (c, d)) = \mathcal{P}_q(a, b) \otimes \mathcal{P}_q(c, d)$ for the space of polynomials in two variables of degree at most q in each variable.

For sufficiently regular functions f and k over the mesh \mathcal{T}_h and $\mathcal{T}_h \times \mathcal{T}_h$, piecewise polynomial approximations k_h, f_h satisfying (7) can be found by appropriate interpolation and choosing the mesh size h small enough. Without further structural assumptions on the data, it seems natural to use uniform grids \mathcal{T}_h , which can be obtained, e.g., by uniform refinement of some reference grid. In Figure 1, we depict the resulting uniform partitions for approximation of the kernel function k .

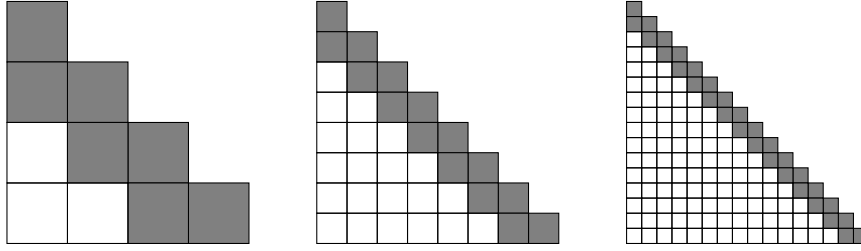


Fig. 1: Uniformly refined grids $\mathcal{T}_h \times \mathcal{T}_h$ for approximation of k . Only the elements required for approximating $k(t, s)$ for $s \leq t$ are depicted. The grid cells near the diagonal $t = s$, i.e., the *nearfield*, play a special role and are thus coloured in gray.

The evaluation of \tilde{y}_h defined by (6) can be split into two contributions

$$\tilde{y}_h(t) = \tilde{w}_h(t) + \tilde{z}_h(t) \quad (11)$$

corresponding to the integrals over the *farfield* and *nearfield* cells, which are depicted in white and gray in Figure 1, respectively. As discussed in the following subsection, the numerical treatment of these contributions differs slightly.

2.3 Practical realisation

From equation (6) and the choice of $f_h \in \mathcal{P}_p(\mathcal{T}_h)$ and $k_h \in \mathcal{P}_{q,q}(\mathcal{T}_h \times \mathcal{T}_h)$, one can see that \tilde{y}_h is a piecewise polynomial of degree $\leq p + q + 1$ over the grid \mathcal{T}_h .

It is often appropriate to replace \tilde{y}_h by a piecewise polynomial $y_h \in \mathcal{P}_p(\mathcal{T}_h)$ with the same degree as the data. For this purpose, we simply choose a set of distinct points $0 \leq \gamma_j \leq 1$, $0 \leq j \leq p$, and define $y_h \in \mathcal{P}_p(\mathcal{T}_h)$ by collocation

$$y_h(t_j^n) = \tilde{y}_h(t_j^n), \quad 0 \leq j \leq p, \quad (12)$$

on every time interval $I^n \in \mathcal{T}_h$, with collocation points $t_j^n = t^{n-1} + \gamma_j h$, $j = 0, \dots, p$. Now let ψ_j^n , $j = 0, \dots, p$, denote the Lagrangian basis of $\mathcal{P}_p(I^n)$ with respect to the interpolation points t_j^n , i.e.,

$$\psi_i^n(t_j^n) = \delta_{i,j}, \quad 0 \leq i \leq p, \quad 1 \leq n \leq N. \quad (13)$$

Then as a consequence of the uniformity of the mesh \mathcal{T}_h , one may deduce that

$$\psi_i^n(t - t^n) = \psi_i^m(t - t^m), \quad 0 \leq i \leq p, \quad 1 \leq m, n \leq N, \quad (14)$$

i.e., the basis $\{\psi_i^n\}_{0 \leq i \leq p}$ is *invariant under translation*, which will become an important ingredient for our algorithm below. The approximate data f_h and the discrete solution y_h can now be expanded as

$$y_h(t) = \sum_{j=0}^p y_j^n \psi_j^n(t), \quad f_h(t) = \sum_{j=0}^p f_j^n \psi_j^n(t), \quad \text{for } t \in I^n. \quad (15)$$

In a similar manner, the approximate kernel function k_h can be expanded with respect to a set of bases $\{\varphi_i^n\}_{i=0, \dots, q}$ for the spaces $\mathcal{P}_q(I^n)$, which leads to

$$k_h(s, t) = \sum_{i=0}^q \sum_{j=0}^q k_{i,j}^{m,n} \varphi_i^m(s) \varphi_j^n(t), \quad \text{for } s \in I^m, \quad t \in I^n. \quad (16)$$

We will again assume translation invariance of this second basis, i.e.,

$$\varphi_i^n(t - t^n) = \varphi_i^m(t - t^m), \quad 0 \leq i \leq q, \quad 1 \leq m, n \leq N. \quad (17)$$

Note that we allow for different polynomial degrees $q \neq p$ in the approximations y_h , f_h , and k_h , and hence two different sets of basis functions are required. Evaluating (6) at time $t = t_j^m$ and utilizing (12), we obtain

$$y_h(t_j^m) = \sum_{n=1}^{m-2} \int_{I^n} k_h(t_j^m, s) f_h(s) ds + \int_{t^{m-2}}^{t_j^m} k_h(t_j^m, s) f_h(s) ds, \quad (18)$$

where we used the splitting of the integration domain $(0, t_j^m)$ into subintervals of the mesh \mathcal{T}_h and an additional separation of farfield and nearfield contributions; see Figure 1. By inserting the basis representations (15) and (16) for y_h , f_h , and k_h , the integrals in the farfield contribution can be expressed as

$$\int_{I^n} k_h(t_j^m, s) f_h(s) ds = \sum_{i=0}^q \varphi_i^m(t_j^m) \sum_{k=0}^q k_{i,k}^{m,n} \sum_{r=0}^p \int_{I^n} \varphi_k^n(s) \psi_r^n(s) ds f_r^n. \quad (19)$$

For convenience of presentation, let us introduce the short-hand notations

$$P_{i,j} = \varphi_i^m(t_j^m), \quad Q_{k,r} = \int_{I^n} \varphi_k^n(s) \psi_r^n(s) ds, \quad (20)$$

and note that the corresponding matrices P and Q are independent of the time steps m, n , due to the translation invariance conditions (14) and (17). The result vector y^m containing entries $y_j^m = y_h(t_j^m)$ from (18) can then be expressed as

$$y^m = w^m + z^m \quad (21)$$

with farfield contribution w^m given by

$$w^m = Pu^m, \quad u^m = \sum_{n=1}^{m-2} k^{m,n} g^n, \quad g^n = Qf^n, \quad (22)$$

where $k^{m,n}$ is the matrix containing the entries $k_{i,j}^{m,n}$. Further introducing the symbols $K^{m,n} = Pk^{m,n}Q$, this may be stated equivalently as $w^m = \sum_{n=0}^{m-2} K^{m,n} f^n$. In a similar manner, we may represent the nearfield contribution z^m by

$$z^m = K^{m,m-1} f^{m-1} + K^{m,m} f^m, \quad (23)$$

with appropriate nearfield matrices $K^{m,m-1}, K^{m,m} \in \mathbb{R}^{(p+1) \times (p+1)}$.

We denote by $\mathbf{y}, \mathbf{f} \in \mathbb{R}^{N(p+1)}$ the global vectors that are obtained by stacking the element contributions y^m, f^n together. The computation of \mathbf{y} can then be written as matrix-vector product $\mathbf{y} = \mathbf{K}\mathbf{f}$ with block-matrix $\mathbf{K} \in \mathbb{R}^{N(p+1) \times N(p+1)}$ consisting of blocks $K^{m,n}$ as defined above. A possible block-based implementation of this matrix-vector product can be realized as follows.

Algorithm 1 Evaluation of Volterra integral operators for uniform meshes.

```

for  $m = 1, \dots, N$  do
   $u = 0$ 
  for  $n = 1, \dots, m-2$  do
     $u = u + k^{m,n} g^n$ 
  end for
   $g^m = Qf^m$ 
   $w^m = Pu$ 
   $z^m = K^{m,m-1} f^{m-1} + K^{m,m} f^m$ 
   $y^m = w^m + z^m$ 
end for

```

At first sight, this algorithm may seem a bit more complicated than actually required. In fact, after generating the matrix blocks $K^{m,n} = Pk^{m,n}Q$, the m th component of the result vector could also be simply computed as $y^m = \sum_{n=1}^m K^{m,n} f^n$. The above version, however, is closer to the fast and oblivious algorithm developed in the next section. Moreover, it is *evolutionary*, i.e., the entries of the vector \mathbf{y} are computed one after another, and *oblivious* in the sense that only the blocks f^{m-1} and f^m are needed for the computation of y^m . Note, however, that all auxiliary values $g^n, n = 1, \dots, m-2$ are required to compute the block y^m and therefore have to be kept in memory. This cost will be substantially reduced by appropriate compression in the next section.

2.4 Computational complexity

As indicated above, the computation of y_h according to (18) can be phrased in algebraic form as a matrix-vector product

$$\mathbf{y} = \mathbf{K}\mathbf{f}, \quad (24)$$

with \mathbf{y} and \mathbf{f} denoting the coefficient vectors for y_h and f_h , and a lower block triangular matrix $\mathbf{K} \in \mathbb{R}^{N(p+1) \times N(p+1)}$. Note that the pattern of the matrix \mathbf{K} is structurally the same as that of the tensor-product grid underlying the approximation of the kernel function k ; see Figure 1, with each cell corresponding to block of size $(p+1) \times (p+1)$. Thus, the computation of $\mathbf{y} = \mathbf{K}\mathbf{f}$ will in general require $O(p^2 N^2)$ operations and $O(p^2 N^2)$ memory to store the matrix \mathbf{K} . In addition, we require $O(pN)$ active memory to store two values of f^n and the history of g .

3 Fast and oblivious algorithm

The aim of this section is to introduce a novel algorithm which allows for a simultaneous compression of the matrix \mathbf{K} used for the evaluation of (24) and the history of the data stored in the vectors g^n , $n \geq 1$. The underlying approximation is that of \mathcal{H}^2 -matrix compression techniques [4, 17].

3.1 Multilevel partitioning

For ease of presentation we will assume that the number of time steps is given as $N = 2^L$, $L \in \mathbb{N}$ and define $h = T/N$. Now let $I^{(n;1)} = I^n$ and introduce a hierarchy of nested partitions into subintervals

$$I^{(n;\ell)} = I^{(2n-1;\ell-1)} \cup I^{(2n;\ell-1)}, \quad \ell > 1,$$

of length $2^{\ell-1}h$. Note that the subintervals $I^{(n;\ell)}$ on level $\ell > 1$ are obtained by recursive coarsening of intervals $I^m = I^{(m;1)}$ on the finest level, and ℓ thus refers to the coarsening level; see Figure 2 for a sketch.

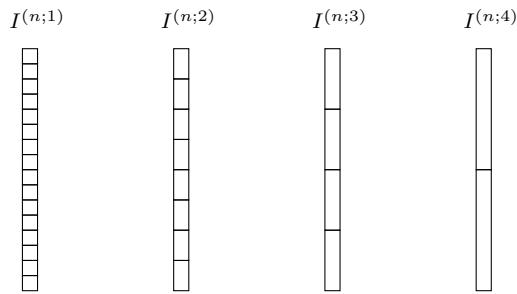


Fig. 2: Mesh hierarchy obtained by recursive coarsening of intervals $I^n = I^{(n;1)}$ with maximal coarsening level $L = 4$ and $N = 2^L = 16$ fine grid cells.

From the hierarchic construction, one can immediately see that

$$I^n \subset I^{(C(n;\ell);\ell)} \quad \text{for} \quad C(n;\ell) := \lceil n/2^{\ell-1} \rceil, \quad (25)$$

where $\lceil r \rceil$ denotes the smallest integer larger or equal to r as usual.

In a similar spirit to [4, 13, 15, 17], we next introduce a multilevel partitioning of the support of the kernel k leading to adaptive hierarchical meshes

$$\begin{aligned} \mathcal{AT}_h = \{ & I^{(m;\ell)} \times I^{(n;\ell)} : \ell = 1 \text{ with } n \in \{m-1, m\} \text{ or} \\ & I^{(m;\ell)} \cap I^{(n;\ell)} = \emptyset \text{ with } I^{(\lceil m/2 \rceil; \ell+1)} \cap I^{(\lceil n/2 \rceil; \ell+1)} \neq \emptyset \}. \end{aligned} \quad (26)$$

Note that every element of \mathcal{AT}_h is square and thus corresponds to one element of a, possibly coarser, uniform mesh $\mathcal{T}_{h'} \times \mathcal{T}_{h'}$. Moreover, any element in \mathcal{AT}_h is the union of elements of the underlying uniform mesh $\mathcal{T}_h \times \mathcal{T}_h$ and can be constructed by recursive agglomeration or coarsening. As illustrated in Figure 3, the

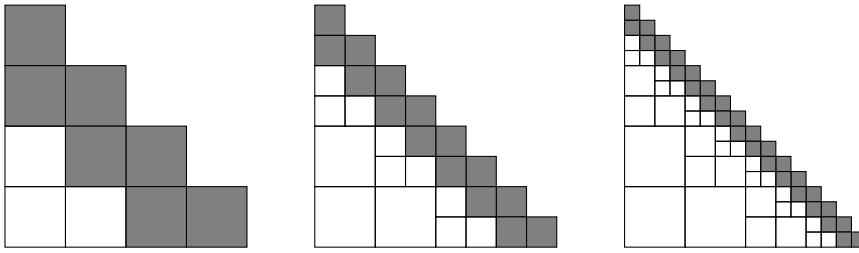


Fig. 3: Adaptive hierarchical meshes \mathcal{AT}_h obtained by recursive coarsening of far fields cells in the corresponding uniformly refined meshes $\mathcal{T}_h \times \mathcal{T}_h$ in Figure 1.

hierarchic adaptive mesh \mathcal{AT}_h can again be split into nearfield elements adjacent to the diagonal and the remaining far field elements. Let us remark that the resulting partitioning and its splitting coincide with most of the classical partitioning strategies developed in the context of panel clustering and \mathcal{H} - and \mathcal{H}^2 -matrices, see [17] and the references therein.

3.2 Adaptive data sparse approximation

Let $\mathcal{P}_{q,q}(\mathcal{AT}_h)$ be the space of piecewise polynomials of degree $\leq q$ in each variable over the mesh \mathcal{AT}_h . Since the adaptive hierarchical mesh is obtained by coarsening of the underlying uniform grid $\mathcal{T}_h \times \mathcal{T}_h$, we certainly have

$$\mathcal{P}_{q,q}(\mathcal{AT}_h) \subset \mathcal{P}_{q,q}(\mathcal{T}_h \times \mathcal{T}_h).$$

Instead of a uniform approximation as used in section 2.2, we now consider adaptive approximations $k_h \in \mathcal{P}_{q,q}(\mathcal{AT}_h)$ for the evaluation of (6) or (18).

Remark 2 Let us assume for the moment that the kernel k in (2) is *asymptotically smooth*, i.e., there exists constants $c_1, c_2 > 0$, $r \in \mathbb{R}$ such that

$$|\partial_t^\alpha \partial_s^\beta k(t, s)| \leq c_1 \frac{(\alpha + \beta)!}{c_2^{\alpha + \beta}} (t - s)^{r - \alpha - \beta} \quad (27)$$

for all $\alpha, \beta \geq 0$ and all $t \neq s$. As shown in [4,17], adaptive approximations $k_h \in \mathcal{P}_{q,q}(\mathcal{AT}_h)$ can be constructed for asymptotically smooth kernels, which converge exponentially in q in the farfield. As a consequence, the same level of accuracy can be achieved by adaptive approximations as with corresponding uniform approximations. In particular, we may assume that the assumptions of lemma 1 are satisfied for the same values of h, N and q . Numerical errors stemming from the hierarchical approximation can therefore be assumed negligible.

Remark 3 It is well-known and not difficult to see that $\dim(\mathcal{P}_{q,q}(\mathcal{T}_h \times \mathcal{T}_h)) = \mathcal{O}(N^2 q^2)$ while $\dim(\mathcal{P}_{q,q}(\mathcal{AT}_h)) = \mathcal{O}(N q^2)$. The adaptive hierarchical approximation thus is *data-sparse* and leads to substantial savings in the memory required for storing the kernel approximation or its matrix representation (24); compare to lemma 3 at the end of this section. In addition, an appropriate reorganisation of the operations required for the matrix-vector product (24) leads to a substantial reduction of computational complexity. Moreover, the fast evaluation also induces an automatic compression of the history of the data.

3.3 Multilevel hierarchical basis

In order to obtain algorithms for the matrix-vector-multiplication (3) of quasi-optimal complexity, we require the following second fundamental ingredient. Based on the multilevel hierarchy $I^{(n;\ell)}$ of time intervals and the translation invariance of the basis functions $\varphi_i^n =: \varphi_i^{(n;1)}$, we define a multilevel basis

$$\varphi_i^{(n;\ell)}(t) = \begin{cases} \sum_{j=0}^q a_{i,j}^{(1)} \varphi_j^{(2n-1;\ell-1)}(t), & t \in I^{(2n-1;\ell-1)}, \\ \sum_{j=0}^q a_{i,j}^{(2)} \varphi_j^{(2n;\ell-1)}(t), & t \in I^{(2n;\ell-1)}, \end{cases} \quad (28)$$

for the spaces $\mathcal{P}_q(I^{(n;\ell)})$, $\ell > 1$ appearing in the far field blocks of the approximation $k_h \in \mathcal{P}_{q,q}(\mathcal{AT}_h)$. Let us note that by translation invariance, the coefficients $a_{i,j}^{(1)}$ and $a_{i,j}^{(2)}$ are independent of n and ℓ .

For each elements $I^{(m;\ell)} \times I^{(n;\ell)} \in \mathcal{AT}_h$, we expand the kernel function as

$$k_h(s, t) = \sum_{i=0}^q \sum_{j=0}^q k_{i,j}^{(m,n;\ell)} \varphi_i^{(m;\ell)}(s) \varphi_j^{(n;\ell)}(t), \quad (s, t) \in I^{(m;\ell)} \times I^{(n;\ell)}. \quad (29)$$

For the computation of the farfield contributions in (18), we can further split the integration domain into

$$[0, t^{m-2}] = \bigcup_{\ell=1}^{L(m)} \bigcup_{n=1}^{B(m;\ell)} I^{(P(m,n;\ell);\ell)} \quad (30)$$

with $L(m) = \lceil \log_2(m) \rceil - 1$, $B(m;\ell) = \text{bin}(m)_\ell + 1$, and $P(m, n; \ell) = C(m; \ell) - n - 1$. Here $\text{bin}(m)_\ell$ denotes the ℓ th digit from behind of the binary representation of m obtained by MATLAB's `dec2bin` function. This partitioning of the integration domain exactly corresponds to the cells of a corresponding row in the adaptive mesh \mathcal{AT}_h ; see Figure 4 for an illustration. More precisely, $L(m) \in \mathbb{N}$ describes the number of different coarsening levels involved in the m th row, $B(m; \ell) \in \{1, 2\}$ corresponds to the number of intervals on each level, and $P(m, n; \ell)$ yields the

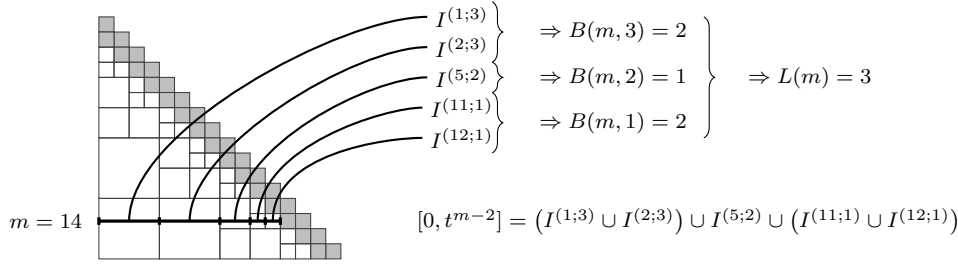


Fig. 4: Illustration of the expressions $L(m)$, $B(m, \ell)$, and $P(m, n; \ell)$ occurring in (30) for $m = 14$ time steps.

indices of these intervals on level ℓ . By inserting the splitting of the integration domain in (30) into equation (18), we obtain

$$y_h(t_j^m) = \sum_{\ell=1}^{L(m)} \sum_{n=1}^{B(m; \ell)} \int_{I^{(P(m, n; \ell); \ell)}} k_h(t_j^m, s) f_h(s) ds + \int_{t^{m-2}}^{t_j^m} k_h(t_j^m, s) f_h(s) ds.$$

We can now further insert the expansions (29) for the kernel k_h into the farfield integrals over $I^{(P(m, n; \ell); \ell)}$ to see that

$$\begin{aligned} \int_{I^{(P(m, n; \ell); \ell)}} k_h(t_j^m, s) f_h(s) ds \\ = \sum_{i=0}^q \varphi_i^{(C(n; \ell); \ell)}(t_j^m) \sum_{k=0}^q k_{i, k}^{(C(n; \ell), P(m, n; \ell); \ell)} g_k^{(P(m, n; \ell); \ell)}, \end{aligned}$$

with auxiliary values

$$g_k^{(P(m, n; \ell); \ell)} = \int_{I^{(P(m, n; \ell); \ell)}} \varphi_k^{(P(m, n; \ell); \ell)}(s) f_h(s) ds.$$

By the recursive definition of $\varphi^{(n; \ell)}$, the latter expression can be rewritten as

$$g_k^{(i; \ell)} = \int_{I^{(i; \ell)}} \varphi_k^{(i; \ell)}(s) f_h(s) ds = \sum_{j=0}^q (a_{i, j}^{(1)} g_k^{(2i-1; \ell-1)} + a_{i, j}^{(2)} g_k^{(2i; \ell-1)})$$

for $\ell > 1$ complemented with $g_k^{(i; 1)} = g_k^i = \sum_{r=0}^p Q_{k, r} f_r^i$ as defined on the uniform grid in Section 2.2. Evaluation of the recursion (28) at time t_j^m further yields

$$\varphi_i^{(C(n; \ell); \ell)}(t_j^m) = \sum_{k=0}^q a_{i, k}^{(B(m, \ell-1))} \varphi_k^{(C(n, \ell-1); \ell-1)}(t_j^m),$$

such that we may define intermediate values

$$u_j^{(C(n; \ell); \ell)} = \sum_{i=0}^q a_{i, j}^{(B(m; \ell))} u_i^{(C(m, \ell+1); \ell+1)} + \sum_{n=1}^{B(m; \ell)} \sum_{k=0}^q k_{i, k}^{(C(n; \ell), P(m, n; \ell); \ell)} g_k^{(P(m, n; \ell); \ell)}.$$

The result of the integral (18) then is finally obtained by

$$y_j^m = y_h(t_j^m) = \sum_{k=0}^q P_{j,k} u_k^{(m;1)} + z^m$$

with nearfield contributions z^m and projections $P_{j,k}$ as given in (20) and (22). The above derivations can be summarized as follows.

Algorithm 2 A fast and oblivious evolutionary algorithm.

```

1: for  $m = 1, \dots, N$  do
2:    $L_{\text{coarse}} = 1 + \lfloor \log_2(\text{bitxor}(m, m-1)) \rfloor$ 
3:   for  $\ell = L_{\text{coarse}}, \dots, 1$  do
4:     if  $B(m; \ell) \neq B(m-1; \ell)$  then
5:        $\mathbf{g}^{(2; \ell)} = \mathbf{g}^{(1; \ell)}$ 
6:       if  $\ell > 1$  then
7:          $\mathbf{g}^{(1; \ell)} = A^{(1)} \mathbf{g}^{(1; \ell-1)} + A^{(2)} \mathbf{g}^{(2; \ell-1)}$ 
8:       else
9:          $\mathbf{g}^{(1; \ell)} = Q \mathbf{f}^{(2)}$ 
10:      end if
11:      Set  $(\mathbf{K}_n)_{i,j} = k_{i,j}^{(C(n; \ell), P(m, n; \ell); \ell)}$  for  $n \in \{1, B(m; \ell)\}$ 
12:       $\mathbf{u}^\ell = \mathbf{K}_1 \mathbf{g}^{(1; \ell)}$ 
13:      if  $B(m; \ell) = 2$  then
14:         $\mathbf{u}^\ell = \mathbf{u}^\ell + \mathbf{K}_2 \mathbf{g}^{(2; \ell)}$ 
15:      end if
16:       $\mathbf{u}^\ell = \mathbf{u}^\ell + A^{(B(m; \ell))} \mathbf{u}^{(\ell+1)}$ 
17:    end if
18:  end for
19:   $\mathbf{f}^{(2)} = \mathbf{f}^{(1)}$ 
20:   $\mathbf{f}_j^{(1)} = f(t_j^m)$ ,  $j = 0, \dots, p$ 
21:   $z^m = N^{m, m-1} \mathbf{f}^{(2)} + N^{m, m} \mathbf{f}^{(1)}$ 
22:   $y^m = P \mathbf{u}^{(1)} + z^m$ 
23: end for

```

The MATLAB function `bitxor(a, b)` returns the integer generated by a bit-wise xor comparison of the binary representation of a and b in $\mathcal{O}(1)$ complexity. It is used to compute the maximum level $L_{\text{coarse}} = \arg \max_k \{B(m; k) \neq B(m-1; k)\}$ in which a coarsening of the intervals happens at step m . Let us note that only one value $u^{(n; \ell)}$ and two values of $g^{(n; \ell)}$ are required for each level ℓ . Moreover, at most two values of f^n are required at any timestep. The required buffers are denoted by $\mathbf{u}^{(\ell)}$, $\mathbf{f}^{(i)}$, and $\mathbf{g}^{(i; \ell)}$, $i = 1, 2$, $\ell = 1, 2, 3, \dots$. The complexity of the overall algorithm is analyzed in detail in the next section.

3.4 Complexity estimates

In the following, we consider Algorithm 2 for the evaluation of (18) with approximate kernel $k_h \in \mathcal{P}_{q,q}(\mathcal{AT}_h)$ and data $f_h \in \mathcal{P}_p(\mathcal{T}_h)$, and with $N = 2^L$ denoting the number of time intervals in \mathcal{T}_h . The assertions of the following two lemmas are well-known, see e.g. [4], but their reasoning is simple and illustrative such that we repeat it for the convenience of the reader.

Lemma 2 *Algorithm 2 can be executed in $\mathcal{O}(N(p^2 + q^2))$ operations.*

Proof The algorithm rearranges the operations of a standard \mathcal{H}^2 -matrix-vector multiplication without adding any significant operations. We therefore simply estimate the complexity of the corresponding \mathcal{H}^2 -matrix-vector multiplication. Let us first remark that the computation of z^m in line 21 requires $\mathcal{O}(p^2)$ operations in each time step. Second, on a given level ℓ , we have to perform $\mathcal{O}(2^\ell)$ applications of $A^{(1)}$ and $A^{(2)}$ in total for obtaining the $g^{(n;\ell)}$ from the ones on level $\ell - 1$, see line 7. Similarly, $\mathcal{O}(2^\ell)$ applications of $A^{(B(m;\ell))}$ in line 16 are in total required on level ℓ for the computation of the $u^{(n;\ell)}$ and $\mathcal{O}(2^\ell)$ multiplications by $k^{(k,n;\ell)}$ need to be performed in lines 12 and 14. Finally, $\mathcal{O}(N)$ values of $g^n = Qf^n$ and $Pu^{(1)}$ need to be computed in line 9 and line 22. Summing up yields

$$\mathcal{O}(Np^2) + 3 \sum_{\ell=1}^L \mathcal{O}(2^{L-\ell})\mathcal{O}(q^2) + 2\mathcal{O}(Npq) = \mathcal{O}(Np^2) + \mathcal{O}(2^L q^2) + \mathcal{O}(Npq),$$

and since $N = 2^L$ this already yields the assertion. \square

Lemma 3 *The \mathcal{H}^2 -matrix representation \mathbb{K} of the adaptive hierarchic approximation $k_h \in \mathcal{P}_{q,q}(\mathcal{AT}_h)$ can be stored in $\mathcal{O}(N(p^2 + q^2))$ memory. If the kernel is of convolution type (4), then the memory cost reduces to $\mathcal{O}(p^2 + \log_2(N)q^2)$.*

Proof The proof for the general adaptive approximation is similar to the previous lemma. For a kernel of convolution type, the hierarchical approximation provides a block Toeplitz structure, such that we only have to store $\mathcal{O}(1)$ coefficient matrices per level for the farfield and $\mathcal{O}(1)$ coefficient matrices for the nearfield. \square

Let us finally also remark on the additional memory required during execution.

Lemma 4 *The active memory required for storing the data history required for Algorithm 2 is bounded by $\mathcal{O}(q \log_2 N + p)$.*

Proof We require $\mathcal{O}(1)$ vectors of length p for the nearfield and at most two vectors $g^{(n;\ell)}$ of length q on $L = \log_2(N)$ levels for the farfield contributions. \square

3.5 Summary

In this section, we discussed the adaptive hierarchical data sparse approximation for the dense system matrix \mathbb{K} in (3) stemming from a uniform polynomial-based discretization of the Volterra-integral operators (2). This approximation amounts to an \mathcal{H}^2 -matrix compression of the system matrix, leading to $\mathcal{O}(N)$ storage complexity for instationary and $\mathcal{O}(\log(N))$ storage complexity for stationary kernel functions. Using a multilevel basis representation on the hierarchy of the time intervals, we formulated a fast and oblivious evolutionary algorithm for the numerical evaluation of Volterra integrals (2). The overall complexity for computing the matrix-vector product in (3) is $\mathcal{O}(N)$ and only $\mathcal{O}(\log(N))$ memory is required to store the compressed history of the data. The algorithm is executed in an oblivious and evolutionary manner and can therefore be generalized immediately to integro-differential equations of the form (1). Moreover, knowledge of the number of time steps N is not required prior to execution.

4 Approximation in the frequency domain

In many interesting applications, see [25] for examples and references, the kernel function in (5) is of convolution type

$$k(t, s) = k(t - s) \quad (31)$$

and only accessible indirectly via its Laplace transform, i.e., the transfer function

$$\hat{k}(s) := (\mathcal{L}k)(s) := \int_0^\infty e^{-st} k(t) dt, \quad s \in \mathbb{C}.$$

At least formally, the evaluation of the kernel function in time domain can then be achieved by the inverse Laplace transform

$$k(t) = (\mathcal{L}^{-1}\hat{k})(t) = \frac{1}{2\pi i} \int_\Gamma e^{t\lambda} \hat{k}(\lambda) d\lambda, \quad t > 0, \quad (32)$$

where Γ is an appropriate contour connecting $-i\infty$ with $i\infty$; see [2] for details.

To ensure the existence of the inverse Laplace transform, we make some technical assumptions and require that

$$\hat{k}(\lambda) \text{ is analytic in a sector } |\arg(\lambda - c)| < \varphi, \quad \frac{\pi}{2} < \varphi < \pi, \quad (33)$$

$$\text{and } |\hat{k}(\lambda)| \leq M|\lambda|^{-\mu} \text{ for some fixed } M, \mu > 0, \quad (34)$$

and that the contour Γ lies within the domain of analyticity of the function K . In this section, we show how to extend Algorithm 2 to this setting and we compare to other approaches proposed in the literature.

4.1 Lubich's convolution quadrature

An efficient approach for the numerical evaluation of Volterra integral operators of convolution type is due to Lubich [23, 24]. Following the exposition of [30], let us briefly recall the basic ideas. Inserting (31) and (32) into (5) and formally interchanging the order of the integrals leads to the expression

$$y(t) = \frac{1}{2\pi i} \int_\Gamma \hat{k}(\lambda) \underbrace{\int_0^t e^{(t-s)\lambda} f(s) ds}_{=: z(t; 0, \lambda)} d\lambda, \quad t \in [0, T]. \quad (35)$$

By comparison with the variation-of-constants formula, one can see that $z(t; 0, \lambda)$ is the unique solution of the initial value problem

$$\frac{d}{dt} z(t; 0, \lambda) = \lambda z(t; 0, \lambda) + f(t), \quad z(0; 0, \lambda) = 0. \quad (36)$$

A discretisation of this problem by the implicit Euler time-stepping scheme with uniform step-size h and time steps $t^n = nh$, $n \geq 0$, leads to approximations

$$z^n(\lambda) := h \sum_{\ell=0}^n \frac{1}{(1 - h\lambda)^{\ell+1}} f(t^{n-\ell}) \approx \int_0^{t^n} e^{\lambda s} f(t^n - s) ds. \quad (37)$$

Higher-order Runge-Kutta schemes or multi-step methods, could be considered in a similar manner [26]. Inserting the approximation (37) into (35) yields

$$y(t^n) \approx y_h(t^n) := \sum_{\ell=0}^n \omega_\ell f(t^{n-\ell}) \quad \text{with} \quad \omega_\ell = \left(\frac{h}{2\pi i} \int_{\Gamma} \frac{\hat{k}(\lambda)}{(1-h\lambda)^{\ell+1}} d\lambda \right). \quad (38)$$

Let us set $y_m = y_h(t^m)$, $f_n = f(t^n)$, and $K_{m,n} = \omega_{m-n}$ for $n \leq m$. Then the discretisation of the convolution integral (5) can be seen to be in the form (24). By Cauchy's integral formula and a change of variable, one can see that

$$\omega_\ell = \frac{1}{2\pi i} \int_{|\lambda|=\rho} \frac{\hat{k}\left(\frac{1-\lambda}{h}\right)}{\lambda^{\ell+1}} d\lambda.$$

An efficient numerical approximation of these integrals can be computed using fast Fourier transforms; see [24, 26] for details. In the same manner, the evaluation of the matrix-vector product (24) can be realized in $O(N \log N)$ operations and requiring $O(N)$ memory to compute and store the weights ω_ℓ and the intermediate results. As outlined in [20], an evolutionary version of the convolution sum can be realized in $O(N \log^2 N)$ complexity.

Before we continue, let us note that the time stepping scheme (37) applied for the discretisation of (36) implicitly utilizes a polynomial, here constant, approximations f_h , y_h on each of the intervals I^n . Therefore, Lubich's convolution quadrature formally fits into the abstract approximations setting considered in Section 2. In the following we show how we can apply the adaptive hierarchical approximation from Section 2 to allow for an $O(N)$ and oblivious evaluation.

4.2 Approximation

As a first step, we show that the convolution kernel k given implicitly by (32) satisfies the assumption (27) on asymptotic smoothness. Thus an accurate adaptive hierarchical approximation as in Section 3 is feasible.

Lemma 5 *Assume that \hat{k} satisfies (33) and (34). Then k as defined in (32) is asymptotically smooth, i.e., it satisfies (27) with $c_2 = \sin(\varphi - \pi/2)$.*

Proof It is sufficient to consider the case $c = 0$ in (33) and $\mu = 1$ in (34). Otherwise, we simply transform $\hat{k}(\lambda + c) = \mathcal{L}(e^{-ct}k(t))(\lambda)$ and $k(t) = k_*^{(\mu-1)}(t)$ with $\hat{k}_*(\lambda) := \mathcal{L}(k_*)(\lambda) = |\lambda|^{\mu-1}\hat{k}(\lambda)$ for $\mu \neq 1$. From [2, Theorem 2.6.1], also see [32], we deduce that k has a holomorphic extension into the sector $|\arg(\lambda)| < \varphi - \pi/2$ with φ as in (33). Thus, the radius of convergence of the Taylor series of k on $t \in (0, \infty)$ is given by $c_2 t$, where $c_2 = \sin(\varphi - \pi/2)$ is independent of t , which implies

$$|\partial_t^\alpha k(t)| \leq c_1 \frac{\alpha!}{c_2^\alpha t^\alpha}$$

for some constant $c_1 > 0$. The chain rule yields (27) which completes the proof.

For the construction of the adaptive approximation k_h , we can now proceed in complete analogy to (11), i.e., we split the convolution integral

$$y_h(t^n) = \int_0^{t^{n-2}} k_h(t^n, s) f_h(s) ds + \int_{t^{n-2}}^{t^n} k_h(t^n, s) f_h(s) ds \quad (39)$$

into a farfield and a nearfield contribution. We note that (32) implies that

$$\int_{t^{n-2}}^{t^n} k_h(t^n, s) f_h(s) ds = \frac{1}{2\pi i} \int_{\Gamma} \hat{k}(\lambda) \underbrace{\int_{t^{n-2}}^{t^n} e^{(t^n-s)\lambda} f_h(s) ds}_{=: z(t^n; t^{n-2}, \lambda)} d\lambda,$$

where $z(t^n; t^{n-2}, \lambda)$ is the solution to (36) with initial data $z(t^{n-2}; t^{n-2}, \lambda) = 0$. The nearfield is thus unchanged when compared to Lubich's original approach.

It remains to deal with the farfield contribution, i.e., the first integral of (39). Following (30), we split $[0, t^{n-2}]$ into subintervals $I^{(n;\ell)}$, each correspond to a certain polynomial approximation. The recursive relations from Section 3.3 thus hold verbatim and only $\mathcal{O}(\log(N))$ storage is needed for the compressed convolution matrix; see lemma 4. Let us note that the coefficient matrices are obtained here by interpolation of the kernel function in time domain. If only the transfer function $\hat{k}(s)$ is accessible, the values of $k_h(t, s) = k(t - s)$ can be computed by fast numerical Laplace inversion; details are given in the following subsection.

Remark 4 Since the approximation f_h is given implicitly by the time stepping scheme, the computation of the $g^{(n;1)} = g^n = Mf^n$ from polynomials may feel a bit artificial. Let us address this concern by remarking that computing

$$g_k^n = \int_{I^n} \varphi_k^n(s - t^{n-1}) f(s) ds$$

is equivalent to solving the differential equation

$$\frac{d}{dt} \tilde{z}_k(t; t^{n-1}, \lambda) = \varphi_k^n(t - t^{n-1}) f(t), \quad \tilde{z}_k(t^{n-1}; t^{n-1}, \lambda) = 0.$$

Solving this problem numerically by a time-stepping scheme can be reformulated as a matrix-vector product $g^n = Mf^n$ where the values f^n coincide with the ones used for the nearfield computations. In this sense, the farfield approximation preserves the structure of the nearfield approximation.

4.3 Numerical Laplace inversion

In the following, we briefly recall some results about the numerical computation of the Laplace inversion formula (32); see [10, 22, 33]. Here we follow the approach of [22, 31] which is based on hyperbolic contours of the form

$$\gamma(\theta) = \mu(1 - \sin(\alpha + i\theta)) + \sigma, \quad \theta \in \mathbb{R}, \quad (40)$$

with $0 < \mu$, $0 < \alpha < \pi/2 - \varphi$, and $\sigma \in \mathbb{R}$, such that the contour remains in the sector of analyticity (33) of \hat{k} . The discretisation of the contour integral (32) by the trapezoidal rule with uniform step with τ yields

$$k(t) \approx \sum_{r=-R}^R \frac{i\tau}{2\pi} e^{\gamma(\theta_r)t} \gamma'(\theta_r) \hat{k}(\gamma(\theta_r)), \quad (41)$$

with $\theta_r = \tau r$. Given we are interested in $k(t)$ for $t \in [t_{\min}, t_{\max}]$ and have fixed values for α and σ , suitable parameters τ and μ are given by

$$\tau = a_\rho(\rho_{\text{opt}}), \quad \mu = \frac{2\pi\alpha R(1 - \rho_{\text{opt}})}{t_{\max} a_\rho(\rho_{\text{opt}})}, \quad \rho_{\text{opt}} = \arg \min_{\rho \in (0,1)} \left(\varepsilon \varepsilon_R(\rho)^{\rho-1} + \varepsilon_R(\rho)^\rho \right),$$

where ε is the machine precision and

$$a_\rho(\rho) = \text{acosh} \left(\frac{t_{\max}/t_{\min}}{(1 - \rho) \sin(\alpha)} \right), \quad \varepsilon_R(\rho) = \exp \left(-\frac{2\pi\alpha R}{a_\rho(\rho)} \right),$$

see [22,31]. In our examples in Section 5 we chose $\alpha = 3/16\pi$, $\sigma = 0$. For error bounds concerning this approach we refer to [22,31].

4.4 A note on the fast and oblivious convolution quadrature

The *fast and oblivious convolution quadrature* (FOCQ) method of [27,31] is also based on the splitting (39) of the convolution integral into nearfield and farfield. The nearfield is again treated in analogy to Lubich's convolution quadrature,

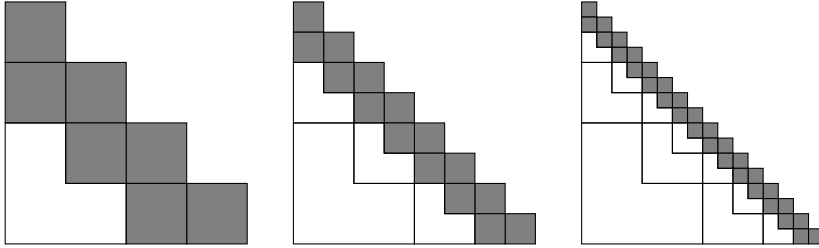


Fig. 5: Hierarchical partitions of fast and oblivious convolution quadrature [31].

whereas the farfield computations are based on a partitioning of $(0, T] \times (0, T]$ into L-shape cells as illustrated in Figure 5. The structure of the partitioning carries over to the convolution matrix K in (24). For given t^m , the farfield integration domain for computing the entry $y_h(t^m)$ is then partitioned into

$$[0, t^{m-2}] = \bigcup_{n=1}^{m-2} I^n = \bigcup_{\ell=1}^{L(m)} \bigcup_{n=1}^{B(m;\ell)} I^{(P(m,n;\ell);\ell)} = \bigcup_{\ell=1}^{L(m)} I_{\text{FOCQ},m}^\ell.$$

Choosing an appropriate contour Γ_ℓ given by (40) and corresponding quadrature points $\theta_r^{(\ell)}$ for each L-shape cell yields an approximation due to (41)

$$\begin{aligned} & \int_{I_{\text{FOCQ},m}^\ell} k(t^m, s) f(s) ds \\ & \approx \frac{i\tau}{2\pi} \sum_{r=-R}^R \hat{k}(\gamma(\theta_r^{(\ell)})) \gamma'(\theta_r^{(\ell)}) e^{\gamma(\theta_r^{(\ell)})(t^m - b^{(\ell)})} \underbrace{\int_{I_{\text{FOCQ},n}^\ell} e^{\gamma(\theta_r^{(\ell)})(b^{(\ell)} - s)} f(s) ds}_{=z(c^{(\ell)}; b^{(\ell)}, \gamma(\theta_r^{(\ell)}))} \end{aligned} \quad (42)$$

with $b^{(\ell)} = \min I_{\text{FOCQ},m}^\ell$, $c^{(\ell)} = \max I_{\text{FOCQ},m}^\ell$, and where $z(c^{(\ell)}, b^{(\ell)}; \gamma(\theta_r^{(\ell)}))$ is the solution to the differential equation (36) with initial condition $z(b^{(\ell)}; b^{(\ell)}, \gamma(\theta_r^{(\ell)})) = 0$. Thus, the fast and oblivious convolution quadrature provides an approximation of the convolution matrix by solving an auxiliary set of $(2R + 1)L$ differential equations. In order to obtain an oblivious algorithm it is crucial that the solution of each differential equation is updated in each time step, i.e., the compressed convolution matrix must be evaluated from *left to right*; see [27, 31] for details.

The connection to our approach is revealed upon noticing that the compression approach underlying the fast and oblivious convolution quadrature actually implements a low-rank approximation in each of the farfields L-shaped blocks, i.e.,

$$\begin{aligned} k(t, s) & \approx \sum_{r=-R}^R \left(\frac{i\tau}{2\pi} e^{\gamma(\theta_r^{(\ell)})(t - b^{(\ell)})} \hat{k}(\gamma(\theta_r^{(\ell)})) \gamma'(\theta_r^{(\ell)}) \right) e^{\gamma(\theta_r^{(\ell)})(b^{(\ell)} - s)} \\ & = \sum_{r=-R}^R U(t, \theta_r^{(\ell)}) V(s, \theta_r^{(\ell)}). \end{aligned}$$

The corresponding farfield approximation (42) thus effectively reads

$$\begin{aligned} \int_{I_{\text{FOCQ},m}^\ell} k(t^n, s) f(s) ds & \approx \sum_{r=-R}^R U(t, \theta_r^{(\ell)}) \int_{I_{\text{FOCQ},m}^\ell} V(s, \theta_r^{(\ell)}) f(s) ds \\ & = \sum_{r=-R}^R U(t, \theta_r^{(\ell)}) z(c^{(\ell)}, b^{(\ell)}, \theta_r^{(\ell)}), \end{aligned}$$

which can be understood as a low-rank matrix-vector product which is realized implicitly by the numerical solution of a differential equation. Since the partitioning Figure 5 can easily be refined to an adaptive partitioning as in Figure 3, the fast and oblivious convolution quadrature can be interpreted as a particular case of an \mathcal{H} -matrix approximation with a particular realisation of the \mathcal{H} -matrix-vector product. The $\mathcal{O}(\log(N))$ memory cost and $\mathcal{O}(N \log(N))$ complexity of the algorithm can then immediately deduced from \mathcal{H} -matrix literature [4, 17].

As mentioned already in the introduction, the algorithm proposed section 3.2 with the modifications discussed above, is based on an \mathcal{H}^2 -matrix approximation and leads to a better complexity of $\mathcal{O}(N)$. It is also clear that the number of quadrature points for the numerical Laplace inversion determines the ranks of the far-field approximations for the \mathcal{H} -matrix approximations, which allows for an improved understanding of the approximation error in terms of the approximation order.

5 Numerical examples

In the following we present a series of numerical examples to illustrate and verify the capabilities of our novel algorithms. The experiments are performed in MATLAB, in which we also implemented a version of the FOCQ for our own reference. Although our new algorithm seems to be considerably faster in all of the following examples we refrain from a comparison since it is well possible that our implementation of the FOCQ is not optimal.

In accordance with the \mathcal{H} - and \mathcal{H}^2 -literature, we require the farfield cells in our implementation to be at least $n_{\min} \times n_{\min} = 16 \times 16$ times larger than the nearfield cells. In our framework, this amounts to constructing the adaptive hierarchical approximation with respect to $H = n_{\min}h$. Following [6, Chapter 2], we choose Radau IIa collocation methods of stage $p = 1, 2, 3$, for the discretization of the Volterra operators, which is exactly the scheme used for the approximation as outlined in section 2.2 and the beginning of section 2.3. This fixes the approximation spaces for y_h and f_h as $\mathcal{P}_p(\mathcal{T}_h)$. The error is measured at the time steps of the coarsest mesh \mathcal{T}_h^c on $[0, T]$, yielding a convergence rate of

$$e_h =: \max_{t_i \in \mathcal{T}_h^c} |y(t_i) - y_h(t_i)| \leq Ch^{2p-1} \quad (43)$$

for $f \in C^{2p-1}([0, T])$ and $k \in C^{2p-1}(\{(t, s) : 0 \leq t \leq s \leq T\})$, cf. [6, Chapter 2]. In the case of Lubich's convolution quadrature this amounts to Runge-Kutta Radau IIa methods and a convergence rate of

$$e_h =: \max_{t_i \in \mathcal{T}_h^c} |y(t_i) - y_h(t_i)| \leq C(h^{2p-1} + h^{p+1+\mu}) \quad (44)$$

for transfer functions satisfying eq. (33) and eq. (34) and $f \in C^{2p-1}([0, T])$, see [26].

5.1 Variation of constants formula

The first example is dedicated to the solution of the differential equation

$$\begin{aligned} y'(t) &= -2ty(t) + 5\cos(5t), \quad t \in (0, 10], \\ y(0) &= 2, \end{aligned} \quad (45)$$

by the variation of constants technique, yielding

$$y(t) = 2e^{-t^2} + 5 \int_0^t e^{s^2-t^2} \cos(5s) \, ds.$$

The integral kernel $k(t, s) = e^{s^2-t^2}$ satisfies the asymptotic smoothness assumption (27), but is not of convolution type. As a reference solution, we solve (45) numerically with a 3-stage Runge-Kutta RadauIIA method and with $N_\infty = 2^{19}$ time steps. For the numerical computations with Algorithm 2, we choose a polynomial degree $q = 16$ for the kernel and various degrees p for the data f and the solution y . The left plot of Figure 6 illustrates that we indeed reach the theoretical convergence rates of the p -stage Radau-IIA method from eq. (43). From the right plot one can immediately deduce the linear complexity of the algorithm.

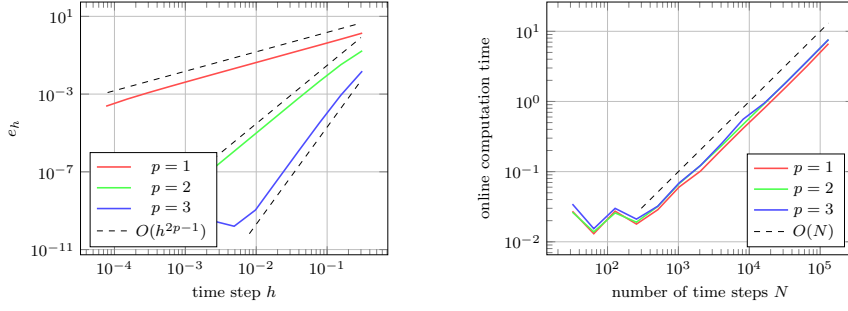


Fig. 6: Approximation errors (left) and computation times (right) for different approximation order p of the underlying discretisation scheme.

5.2 Nonlinear Volterra integral equation

We continue with a second test example taken from [31], in which we consider the nonlinear Volterra integral equation

$$u(t) = - \int_0^t \frac{(u(\tau) - \sin(\tau))^3}{\sqrt{\pi(t-\tau)}} d\tau, \quad t \in [0, 60].$$

In this example, the convolution kernel $k(t-s) = 1/\sqrt{\pi(t-s)}$ is of convolution type, with Laplace transform given by $\hat{k}(\lambda) = 1/\sqrt{\lambda}$. The evaluation of the integral kernel $k(t-s)$ is realized via numerical inverse Laplace transforms with $R = 15$ quadrature points and the kernel is approximated by piecewise polynomials of degree $q = 8$ in the farfield; see section 4. Since the data $f(t, u) = (u - \sin(t))^3$ here depend on u , a nonlinear equation must be solved for each time step for which we employ a Newton method up to a tolerance of 10^{-12} . As reference solution for computing the errors, we here simply take the numerical solution computed on a finer grid. The results of Figure 7 again clearly show the predicted convergence

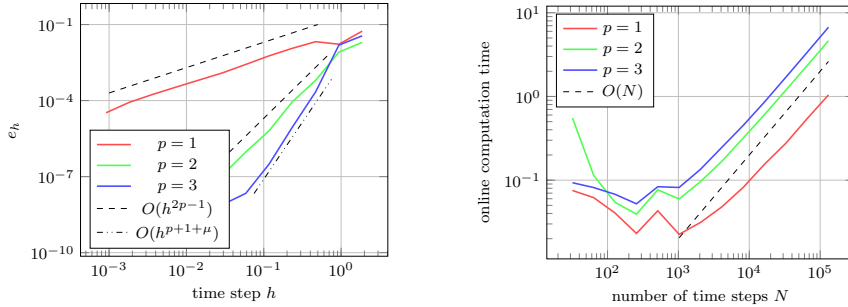


Fig. 7: Approximation errors (left) and computation times (right) for different approximation order p of the underlying discretisation scheme.

rates h , h^2 , and $h^{4.5}$, cf. (44), and the linear complexity of Algorithm 2.

5.3 Fractional diffusion with transparent boundary conditions

As a last example, which is taken from [8,31], we consider the one-dimensional fractional diffusion equation

$$u(x, t) = u_0(x) + \int_0^t \frac{(t - \tau)^{\alpha-1}}{\Gamma(\alpha)} \Delta_x u(x, \tau) d\tau + g(x, t), \quad x \in \mathbb{R}, \quad t \in \mathbb{R}_{>0},$$

with $\alpha = 2/3$, $u(x, \cdot) \rightarrow 0$ for $|x| \rightarrow \infty$ and $g(x, 0) = 0$. For the computations, we restrict the spatial domain to $x \in (-a, a)$, assume that u_0 and g have support in $[-a, a]$, and impose transparent boundary conditions on $x = \pm a$ which read

$$u(x, t) = - \int_0^t \frac{(t - \tau)^{\alpha/2-1}}{\Gamma(\alpha/2)} \partial_{\mathbf{n}} u(x, \tau) d\tau, \quad x = \pm a;$$

we refer to [19,31] for further details on the model. The Laplace transform of the convolution kernel $k(t - s) = (t - s)^{\alpha-1}/\Gamma(\alpha)$ is here given by $\hat{k}(\lambda) = 1/\lambda^\alpha$.

For the spatial discretisation we employ a finite difference scheme on a equidistant mesh $x_i = i\tau$, $\tau = a/M$, $i = -M, \dots, M$ and use second-order finite differences within the domain and central differences to approximate the normal derivative on the boundary; see [8,31]. For the time discretisation we employ the frequency domain version of our algorithm with $R = 30$ quadrature points for the inverse Laplace transform and polynomial degree $q = 16$ for the farfield interpolation. We note that two different convolution quadratures are required, one for the fractional derivative in $(-a, a)$ involving α and one for the fractional derivative of the boundary values, involving $\alpha/2$.

For the space discretisation we consider a fixed mesh with $M = 10^4$ which is fine enough to let the error of the time discretisation dominate. As a reference solution we take method with order $p = 3$ on a finer mesh. Other than in the

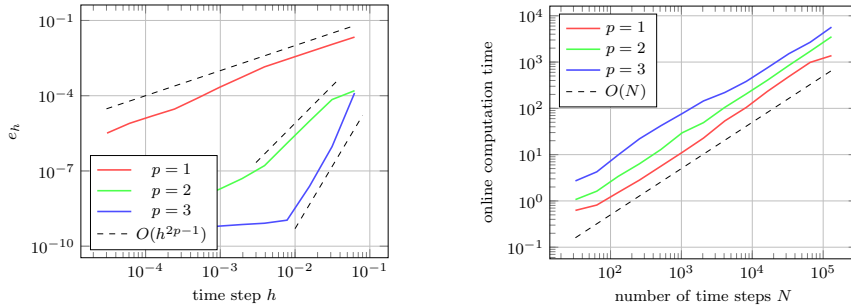


Fig. 8: Convergence plot and computation times for the fractional diffusion problem with transparent boundary conditions.

previous examples, we cannot expect the full order of convergence of the Radau-IIA methods as in eq. (44) due to the lack of temporal smoothness of the solution at $t = 0$; let us refer to [8, Section 1] for further discussion. In Figure 8, we however still observe a very good approximation in the pre-asymptotic phase and a substantial improvement in accuracy when using higher approximation order

p . As predicted by theory, the computation times again increase linearly in the number of time steps.

Funding

Support by the German Science Foundation (DFG) via TRR 146 (project C3), TRR 154 (project C04), and SPP 2256 (project Eg-331/2-1) is gratefully acknowledged.

References

1. S. Amari. Dynamics of pattern formation in lateral-inhibition type neural fields. *Biological Cybernetics*, 27(2):77–87, 1977.
2. W. Arendt, C.J.K. Batty, M. Hieber, and F. Neubrander. *Vector-Valued Laplace Transforms and Cauchy Problems*. Springer Basel, Basel, 2011.
3. D. Baffet and J.S. Hesthaven. A Kernel Compression Scheme for Fractional Differential Equations. *SIAM Journal on Numerical Analysis*, 55(2):496–520, January 2017.
4. S. Börm. *Efficient Numerical Methods for Non-Local Operators*, volume 14 of *EMS Tracts in Mathematics*. European Mathematical Society (EMS), Zürich, 2010.
5. A. Brandt and A.A. Lubrecht. Multilevel matrix multiplication and fast solution of integral equations. *Journal of Computational Physics*, 90(2):348–370, October 1990.
6. H. Brunner. *Collocation Methods for Volterra Integral and Related Functional Differential Equations*. Number 15 in Cambridge Monographs on Applied and Computational Mathematics. Cambridge University Press, Cambridge, UK ; New York, 2004.
7. H. Brunner. *Volterra Integral Equations: An Introduction to Theory and Applications*. Cambridge University Press, Cambridge, 2017.
8. E. Cuesta, C. Lubich, and C. Palencia. Convolution quadrature time discretization of fractional diffusion-wave equations. *Mathematics of Computation*, 75(254):673–697, January 2006.
9. W. Dahmen, S. Prössdorf, and R. Schneider. Wavelet approximation methods for pseudodifferential equations II: Matrix compression and fast solution. *Advances in Computational Mathematics*, 1(3):259–335, October 1993.
10. B. Dingfelder and J.A.C. Weideman. An improved Talbot method for numerical Laplace transform inversion. *Numerical Algorithms*, 68(1):167–183, January 2015.
11. J. Dölz, H. Egger, and V. Shashkov. A convolution quadrature method for Maxwell’s equations in dispersive media, 2020.
12. H. Egger, K. Schmidt, and V. Shashkov. Multistep and Runge–Kutta convolution quadrature methods for coupled dynamical systems. *Journal of Computational and Applied Mathematics*, page 112618, January 2020.
13. W. Fong and E. Darve. The black-box fast multipole method. *Journal of Computational Physics*, 228(23):8712–8725, December 2009.
14. K. Giebermann. Multilevel approximation of boundary integral operators. *Computing*, 67(3):183–207, 2001.
15. L. Greengard and V. Rokhlin. A fast algorithm for particle simulations. *Journal of Computational Physics*, 73(2):325–348, 1987.
16. W. Hackbusch. A sparse matrix arithmetic based on \mathcal{H} -matrices part I: Introduction to \mathcal{H} -matrices. *Computing*, 62(2):89–108, 1999.
17. W. Hackbusch. *Hierarchical Matrices: Algorithms and Analysis*. Springer, Heidelberg, 2015.
18. W. Hackbusch and Z.P. Nowak. On the fast matrix multiplication in the boundary element method by panel clustering. *Numerische Mathematik*, 54(4):463–491, July 1989.
19. T. Hagstrom. Radiation boundary conditions for the numerical simulation of waves. *Acta Numerica*, 8:47–106, January 1999.
20. E. Hairer, Ch. Lubich, and M. Schlichte. Fast Numerical Solution of Nonlinear Volterra Convolution Equations. *SIAM Journal on Scientific and Statistical Computing*, 6(3):532–541, July 1985.

21. S. Kapur, D.E. Long, and J. Roychowdhury. Efficient time-domain simulation of frequency-dependent elements. In *Proceedings of International Conference on Computer Aided Design*, pages 569–573, San Jose, CA, USA, 1996. IEEE Comput. Soc. Press.
22. M. López-Fernández, C. Palencia, and A. Schädle. A Spectral Order Method for Inverting Sectorial Laplace Transforms. *SIAM Journal on Numerical Analysis*, 44(3):1332–1350, January 2006.
23. Ch. Lubich. Convolution quadrature and discretized operational calculus. I. *Numerische Mathematik*, 52(2):129–145, January 1988.
24. Ch. Lubich. Convolution quadrature and discretized operational calculus. II. *Numerische Mathematik*, 52(4):413–425, July 1988.
25. Ch. Lubich. Convolution Quadrature Revisited. *BIT Numerical Mathematics*, 44(3):503–514, August 2004.
26. Ch. Lubich and A. Ostermann. Runge-Kutta methods for parabolic equations and convolution quadrature. *Mathematics of Computation*, 60(201):105–105, January 1993.
27. Ch. Lubich and A. Schädle. Fast Convolution for Nonreflecting Boundary Conditions. *SIAM Journal on Scientific Computing*, 24(1):161–182, January 2002.
28. R. Metzler and J. Klafter. The random walk’s guide to anomalous diffusion: A fractional dynamics approach. *Physics Reports*, 339(1):1–77, December 2000.
29. V. Rokhlin. Rapid solution of integral equations of classical potential theory. *Journal of Computational Physics*, 60(2):187–207, September 1985.
30. F.-J. Sayas. *Retarded Potentials and Time Domain Boundary Integral Equations*, volume 50 of *Springer Series in Computational Mathematics*. Springer International Publishing, Cham, 2016.
31. A. Schädle, M. López-Fernández, and Ch. Lubich. Fast and Oblivious Convolution Quadrature. *SIAM Journal on Scientific Computing*, 28(2):421–438, January 2006.
32. M. Sova. The Laplace transform of analytic vector-valued functions (complex conditions). *Časopis pro pěstování matematiky*, 104(3):267–280, 1979.
33. A. Talbot. The Accurate Numerical Inversion of Laplace Transforms. *IMA Journal of Applied Mathematics*, 23(1):97–120, 1979.